

## Channel Spectral Separation Narrowing for Spectral Beam Combining by Apodisation of the Reflecting Volume Bragg Grating

Shen Benjian\*, Tan Jichun, Zheng Guangwei, and He Yanlan

*National University of Defence Technology, Changsha 410073*

*\*E-mail: shenbenjian@163.com*

### ABSTRACT

The sidelobe in diffraction efficiency of reflecting volume Bragg grating (RVBG) limits the wavelength channel spectral separation, which determines the combining power output in spectral beam combining (SBC) systems. A novel SBC system based on the apodised RVBG has been proposed to suppress the sidelobe. Several apodised RVBGs have been compared and the optimal apodised RVBG is obtained by using the chain-matrix approach. Numerical results show that the sidelobe could be suppressed excellently with Blackman apodised RVBG. In the numerical example, the minimal channel spectral separation was 1.0 nm for SBC system based on the RVBG and it decreased to 0.6 nm for the novel SBC system based on the Blackman apodised RVBG when the spectral combining efficiency of both systems achieves the same maximum value.

**Keywords:** High power laser, spectral beam combining, channel spectral separation narrowing, sidelobe suppression, apodised volume Bragg grating

### 1. INTRODUCTION

High average power output laser systems are useful in directed energy applications. However, maximum power emitted by a single solid-state laser is limited by the thermo-optic effects<sup>1</sup>. It is an effective approach to get high power laser output by combining multiple lasers into a single beam<sup>2,3</sup>. There are two approaches for beam combining—coherent and incoherent. A comparative review of those approaches is presented by Fan and Sanchez<sup>4</sup>. The main challenge of coherent combining is precise control of wavelengths and relative phases of each laser, especially the relative phase noise between channels<sup>5</sup>, which make coherent combining of multiple lasers difficult to obtain. However, these problems can be avoided by incoherent combining technologies.

Spectral beam combining (SBC) is a typical approach of incoherent combining<sup>6</sup>, which is based on the diffractive elements such as reflecting volume Bragg grating (RVBG) that combines multiple lasers at different wavelengths into a single diffraction-limited beam in the near- and far-fields. The output power of SBC is determined by the number of wavelength channels, and high average power laser output can be obtained by spectrally combining multiple lasers. For example, consider a laser system operating within a 10 nm total spectral bandwidth. 10-kW-level laser output can be obtained by combining 20 lasers with channel spectral separation of 0.5 nm and 500 W output power of each laser. However, the total bandwidth for SBC is determined by the application requirements. Increasing the number of wavelength channels in a given spectral range requires decreasing the channel spectral separation,

but the channel spectral separation is limited by the sidelobe in diffraction efficiency. Suppressing the sidelobe is an effective approach to decrease channel spectral separation. However, it was found that there has been no research reporting on this subject in SBC systems.

In the fibre Bragg gratings, the sidelobe in diffraction efficiency is well suppressed by the apodisation technologies. The apodisation technologies into the RVBG have been introduced to suppress the sidelobe in diffraction efficiency for SBC. The difference between these two apodisation technologies is that the beam is normally incidence in fiber Bragg grating but obliquely incidence on the RVBG for the SBC system. In this paper, a novel SBC system based on the apodised RVBG is proposed to suppress the sidelobe and decrease channel spectral separation.

### 2. THEORETICAL MODEL

The scheme of SBC based on apodised RVBG is illustrated in Fig. 1. The grating boundary normals are in the  $z$  direction, and the grating vector is in the  $yo$ z plane, and the constant refractive index is described by the pattern which parallels the  $xoy$  plan. The grating extends from  $z=0$  to  $z=d$  where  $d$  is the grating thickness. The parameters described in Fig. 1 are:  $\theta_i$ —incident angle;  $\theta_r$ —refraction angle in the grating;  $\mathbf{K}$ —grating vector with module  $|\mathbf{K}|=2\pi/\Lambda$ ;  $\Lambda$ —grating period;  $\lambda_i$ —incident beam at Bragg wavelength;  $\Delta\lambda$ —spectral separation;  $z$ —direction along grating thickness;  $n_1$  and  $n_3$  is the refractive index of the medium in region 1 ( $z<0$ ) and region 3 ( $z>d$ ), respectively;  $n_2$ —refractive index of the volume Bragg grating.

The refractive index distribution of the un-slanted apodised RVBG (grating vector perpendicular to the grating surface) along the grating thickness is<sup>7</sup>

$$n_z = n_0 + n(z) \cos(\mathbf{K}z) \quad (1)$$

where  $n(z)$  is the apodised function.

In the following, the apodised functions are

$$n(z) = \begin{cases} n_m \tanh(8z/d) & 0 \leq z \leq d/2 \\ n_m \tanh[8(d-z)/d] & d/2 \leq z \leq d \end{cases} \quad \text{Tanh4x}$$

$$\begin{aligned} n(z) &= n_m [1 - (2x)^2] / (1 - x^2) && \text{Cauchy} \\ n(z) &= n_m [1 + 0.5 \cos(2\pi x)] / 1.5 && \text{Hamming} \\ n(z) &= n_m [1 + 1.19 \cos(2\pi x) + 0.19 \cos(4\pi x)] / 2.38 && \text{Blackman} \end{aligned} \quad (2)$$

where  $x = (z - d/2)/d$ ,  $n_m$  is the maximum of refractive index modulation.

In Fig. 1, the reflected beam at Bragg wavelength  $\lambda_1$  is obliquely incident from region 1 on the left surface of the grating at angle  $\theta_i$  in the  $yo$ z plane, and diffract with high diffraction efficiency because the Bragg condition is satisfied. The transmitted beam at wavelength  $\lambda_2 = \lambda_1 + \Delta\lambda$  is incident from region 3 on the right surface of the grating at the same angle and incident plane with  $\lambda_1$ , and transmits the grating. In region 1, the two beams are power added and spatially overlapped in the near- and far-field. For achieving a high combining efficiency to ensure a high combining power output, the diffraction efficiency for  $\lambda_1$  and the transmission efficiency for  $\lambda_2$  should be high.

For analysing the diffraction efficiency of the volume Bragg grating, the volume Bragg grating is decomposed into a large number of sufficiently thin slabs. The amplitude of the incident and the reflected electric field at the input plan ( $z=0$ ) can be related to those at output plan ( $z=d$ ) by the following relations<sup>8</sup>

$$\begin{pmatrix} 1 \\ E_r \end{pmatrix} = \prod_{i=1}^N \begin{pmatrix} A_i & B_i \\ B_i^* & A_i^* \end{pmatrix} \times \frac{1}{\tau_{N+1}} \begin{pmatrix} 1 & r_{N+1} \\ r_{N+1} & 1 \end{pmatrix} \begin{pmatrix} E_t \\ 0 \end{pmatrix} \quad (3)$$

where  $N$  is the number of thin slabs,  $E_r$  and  $E_t$  are the normalised electric field amplitude of the reflected and transmitted beams, respectively. The matrix elements are

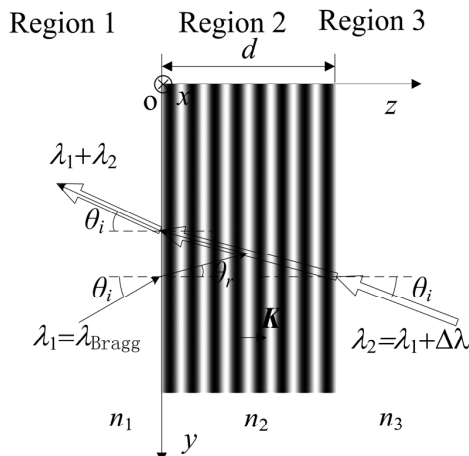


Figure 1. Scheme of SBC systems based on apodised RVBG.

$$A_i = (1/\tau_i) \exp(j2\pi n_{2,i} d_i \cos\theta_{2,i} / \lambda) \quad (4)$$

$$B_i = r_i A_i^* \quad (5)$$

where  $\lambda$  is the free-space wavelength of incident beam,  $n_{2,i}$ ,  $\theta_{2,i}$ ,  $d_i$ ,  $r_i$  and  $\tau_i$  are the refractive index, the refraction angle, the thickness, the amplitude of reflection and transmission coefficients of the  $i^{\text{th}}$  slab, respectively. The diffraction (reflectance) efficiency is:  $\eta = E_r E_r^*$ .

### 3. SIMULATION RESULTS

#### 3.1 Optimal Apodised RVBG for Sidelobe Suppression

In the simulation, H-mode polarisation (electric field perpendicular to the plane of incidence) beam was taken as an example, the grating period  $\Lambda = 0.36 \mu\text{m}$ , the Bragg wavelength  $\lambda_1 = 1064 \text{ nm}$  is obliquely incident on the grating at angle  $\theta_1 \approx 9.8^\circ$ . It was assumed that the media in region 1 and region 3 are homogenous and lossless medium with refractive index  $n_0 = 1.5$  and we divide each period of the grating was divided into 25 slabs. In the given simulation conditions, the computed diffraction efficiency tends to be a constant value with the increasing of the number of slabs. The diffraction efficiency precision can be estimated better than 1%.

In calculation, it was found that the peak diffraction efficiency of the apodised RVBG could be given as

$$\eta_{\max} = \tanh^2(\pi a_{\text{eff}} n_m d / \lambda \cos\theta_r) \quad (6)$$

where  $a_{\text{eff}}$  is the apodisation parameter which is defined as that in the fiber Bragg grating<sup>9</sup>

$$a_{\text{eff}} = \int_0^d z n(z) dz / \int_0^d z dz \quad (7)$$

For RVBG,  $a_{\text{eff}} = 1$ . The apodisation parameter values of the apodised RVBG considered in this analysis are listed in Table 1.

For securing higher than 99.9 per cent of the peak diffraction efficiency, the products  $-a_{\text{eff}} n_m d$  should be larger than  $1.4 \times 10^{-6}$  from Eqn (6). A concise comparison of spectral diffraction efficiency between the RVBG and the apodised RVBG is shown in Fig. 2, when the products  $-a_{\text{eff}} n_m d$  is equal to  $1.4 \times 10^{-6}$  and  $d = 5 \text{ mm}$ . The location of the first sidelobe of each grating is marked except the Blackman apodised RVBG due to neglectable value comparing to others.

In Fig. 2, it is shown that the sidelobe in diffraction efficiency of the apodised RVBG described above is smaller

Table 1. Apodisation parameter with different apodisation profiles

Apodisation profile $n(z)$	Apodisation parameter $(a_{\text{eff}})$
Tanh	0.8268
Cauchy	0.7042
Hamming	0.6667
Blackman	0.4202

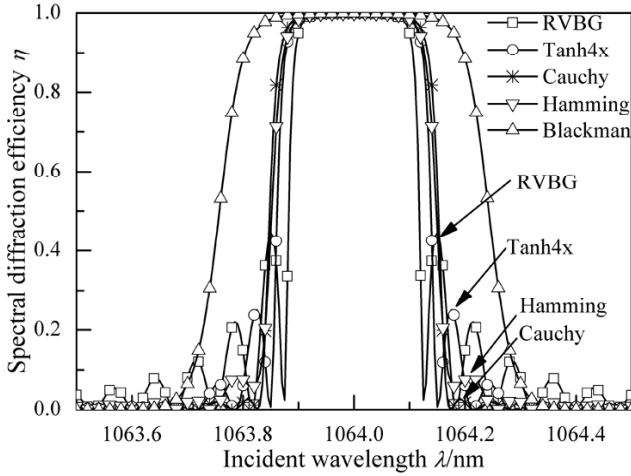


**Figure 2. Comparison of spectral diffraction efficiency between the RVBG and the apodised RVBG.**

than that of the RVBG. The peak diffraction efficiency of the first sidelobe is larger than that of the high orders, and the bandwidth for high diffraction efficiency of the apodised RVBG is broader than that of RVBG, which will be considered in Section 3.2. To choose the optimal apodised RVBG for sidelobe suppression, the peak diffraction efficiency of the first sidelobe was compared with different grating described above, and it was found that the peak diffraction efficiency of the first sidelobe is determined by the products  $-a_{eff} n_m d$ . The relationship is shown in Fig. 3.

In Fig. 3, the value of the peak diffraction efficiency of the first sidelobe is increased with the increase of the products except the Cauchy apodised RVBG. The first sidelobe of the Blackman apodised RVBG is the smallest and was under  $10^{-5}$ -level. Although the peak diffraction efficiency of the first sidelobe for Cauchy apodised RVBG was decreased with increase of the products  $-a_{eff} n_m d$  when these were larger than  $1.0 \times 10^{-6}$ , the effect of the second sidelobe became comparable or even larger than that of the first sidelobe. So the Blackman apodised RVBG is an excellent candidate for sidelobe suppression.

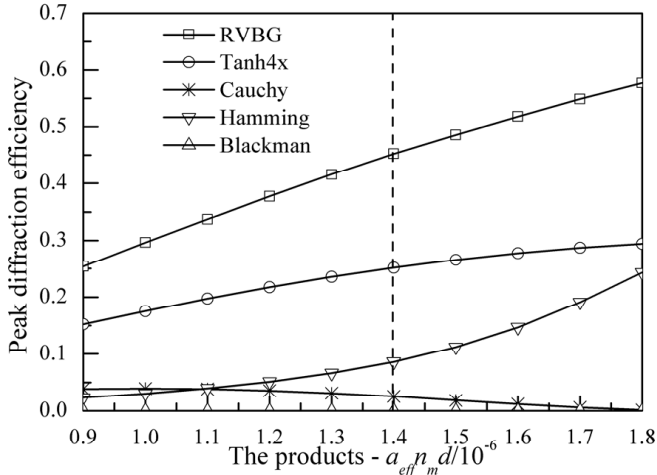


**Figure 3. The peak diffraction efficiency of the first sidelobe vs the products  $-a_{eff} n_m d$ .**

### 3.2 Spectral Selectivity of Blackman Apodised RVBG

Beams emitted by lasers have spectral width which might be equal or might exceed the spectral selectivity full width at half maximum (FWHM) of grating, this competition leads to decreasing the reflectance and transmittance of beams, and also the combining efficiency. For the RVBG, the spectral selectivity can be optimised by changing the grating thickness for achieving high reflectance and transmittance of the beams. However, for the Blackman apodised RVBG, whether the spectral selectivity can be optimised by the same approach or not, should be analysed. The spectral selectivity of the RVBG and the Blackman apodised RVBG as a function of its thickness is shown in Fig. 4 when the peak diffraction efficiency is 99.9 per cent, i.e., the products  $-a_{eff} n_m d$  was kept equal to  $1.4 \times 10^{-6}$ .

In Fig. 4, spectral selectivity of the grating was decreased with increasing of its thickness, and the spectral selectivity of the Blackman apodised RVBG was broader than that of RVBG at the same grating thickness. By optimising the grating thickness and the maximum of the refractive index modulation, both gratings could achieve the same peak diffraction efficiency and the same spectral selectivity for achieving high combining efficiency.

### 3.3 Channel Spectral Separation Narrowing

To make a clear understanding about the advantage of sidelobe suppression to channel spectral separation narrowing, a two-beam SBC system was taken as a numerical example. The Bragg wavelength was 1064 nm which was emitted by the Nd:YAG laser, and the wavelength of the transmitting beam was emitted by another Nd:YAG laser which is temperature tuning for emitting an expected wavelength<sup>10</sup>. The spectral width (HWE<sup>-2</sup>M, half width at  $e^{-2}$  maximum) of the two beams was 0.2 nm by controlling the optical resonator. The spectral selectivity of the grating was chosen as 0.4 nm for achieving the diffraction efficiency of the incident beam approaches to 95 per cent. Under this condition, the optimal parameters of the grating were  $d=3.04$  mm,  $n_m=461$  ppm (1 ppm= $10^{-6}$ ) for RVBG, and

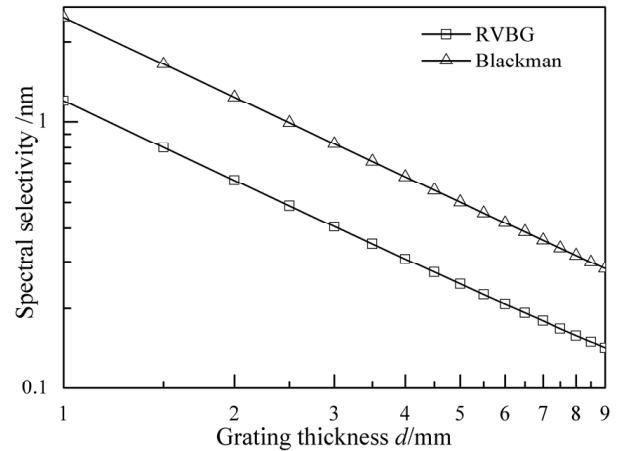


**Figure 4. Spectral selectivity of grating as a function of grating thickness.**

$d=6.29$  mm,  $n_m=531$  ppm for Blackman apodised RVBG from Fig. 4.

Considering a Gaussian shape spectral distribution of the beams emitting by lasers as

$$G(\lambda)=\exp[-2(\lambda-\lambda_0)^2/\omega^2] \quad (8)$$

where  $\lambda_0$  is the centre wavelength and  $\omega$  is the spectral width of the beams. The reflection and transmission efficiency of the beams were

$$\eta_D(\lambda_1)=\int G(\lambda)\eta(\lambda)d\lambda/\int G(\lambda)d\lambda \quad (9)$$

$$\eta_T(\lambda_2)=\int G(\lambda)[1-\eta(\lambda)]d\lambda/\int G(\lambda)d\lambda \quad (10)$$

where  $\eta(\lambda)$  represents spectral diffraction efficiency of the grating at wavelength  $\lambda$  and angle  $\theta$ , which is the incident angle of Bragg wavelength,  $\lambda_1$  and  $\lambda_2$  is the center wavelength of the reflecting and transmitting beams, respectively. The spectral combining efficiency is the ratio of the combining output power to the total input power. Assuming that the two beams have the same output power, the combining efficiency is

$$\eta_{ce}=[\eta_D(\lambda_1)+\eta_T(\lambda_2)]/2 \quad (11)$$

Figure 5 shows that the combining efficiency increases with the increase of spectral separation between the two incident beams and tends to be a constant value for large spectral separation. In Fig. 5, it is shown that the combining efficiency increases with the increase of channel spectral separation and be a constant value at large channel spectral separation for the SBC system based on the RVBG or based on the Blackman apodised RVBG. The maximum value of the combining efficiency was 96.8 per cent for both the systems in this numerical example. For the SBC system based on the RVBG, the minimal spectral separation between channels was 1.0 nm for achieving the combining efficiency at this maximum value. However, for the SBC system based on the Blackman apodised RVBG, the minimal spectral separation between channels was decreased to 0.6 nm for the same combining efficiency as that based on the RVBG. In a given total spectral bandwidth, the number of channels for the SBC system is equal to the ratio of the total spectral

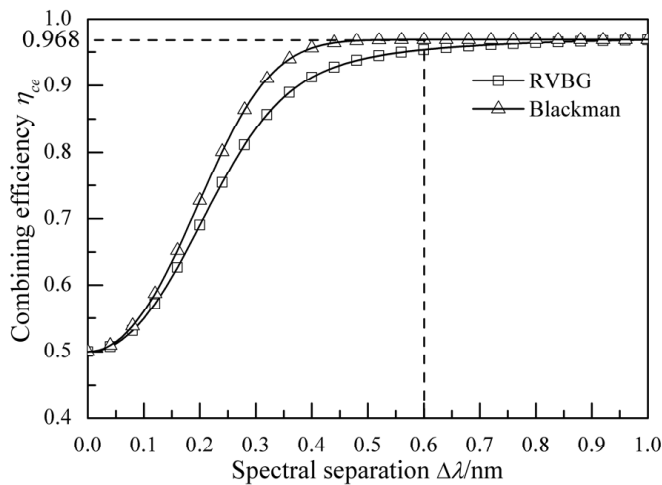


Figure 5. Effect of spectral separation on spectral combining efficiency.

bandwidth to the minimal spectral separation between the channels. The number of channels for SBC system based on the Blackman apodised RVBG is 1.7 times larger than that based on the RVBG, then this novel SBC system has great potential to achieve higher power laser output based on the fact that the output power of the SBC is proportional to the number of channels.

#### 4. CONCLUSIONS

In conclusion a novel SBC system based on apodised RVBG to suppress the sidelobe in diffraction efficiency of the grating and to decrease the channel spectral separation. Numerical results show that the sidelobe is suppressed excellently with Blackman apodised RVBG, and this grating is an excellent combiner candidate for SBC system. The minimal channel spectral separation is 1.0 nm for the SBC system based on the RVBG and it decrease to 0.6 nm for the novel SBC system based on the Blackman apodised RVBG. The feature of channel spectral separation narrowing makes this novel system to be an excellent candidate for achieving high power laser output.

#### ACKNOWLEDGEMENT

The project is supported by NSAF Foundation of National Natural Science Foundation of China and Chinese Academy of Engineering Physics (Grant No. 10676038).

#### REFERENCES

1. Fan, T.Y. Laser beam combining for high-power, high-radiance sources. *IEEE J. Selected Topics Quant. Electro.* 2005, **11**(3), 567-77.
2. Sevian, A.; Andrusyak, O. & Ciapurin, I. Ultimate efficiency of multi-channel spectral beam combiners by means of volume Bragg gratings. *SPIE*, 2007, **64530R**, 1-8.
3. Chann, B.; Huang, R. K. & Missaggia, L. J. Near-diffraction-limited diode laser arrays by wavelength beam combining. *Optics Letters*, 2005, **30**(16), 2104-106.
4. Fan, T. Y. & Sanchez, A. Coherent (phased array) and wavelength (spectral) beam combining compared. *SPIE*, 2005, **5709**, 157-64.
5. Andrusyak, O.; Smirnov, V. & Venus, G. Beam combining of lasers with high spectral density using volume Bragg gratings. *Optics Communications*, 2009, **282**, 2560-563.
6. Andrusyak, O.; Ciapurin, I. & Sevian, A. Power scaling of laser systems using spectral beam combining with volume bragg gratings in PTR glass. In conference on lasers and electro-optics/quantum electronics and laser science conference and photonic applications systems technologies, OSA Technical Digest Series (CD) (Optical Society of America, 2007), Paper JTua85.
7. Pastor, D.; Capmany, J. & Ortega, D. Design of apodised linearly chirped fiber gratings for dispersion compensation. *J. Lightwave Technol.*, 1996, **14**(11), 2581-588.
8. Moharam, M. G. & Gaylord, T. K. Chain-matrix analysis of arbitrary-thickness dielectric reflection gratings. *J. Opti. Society America*, 1982, **72**(2), 187-90.

9. Cross, P.S. & Kogelnik, H. Sidelobe suppression in corrugated-waveguide filters. *Optics Letters*, 1977, **1**(1), 43-45.
10. Koechner, W. Solid-State Laser Engineering (Sixth Revised and Updated Edition). William T. Rhodes, U.S.A, 2006. 268 p.

#### Contributors



**Mr Shen Benjian** obtained his BS in Physics from National University of Defense Technology in 2007. He is currently a PhD candidate at the National University of Defense Technology, College of Science, and his main research field is beam combining technologies and volume Bragg grating designing.



**Prof Tan Jichun** received his MS from Sichuan University, and presently he is a Professor at the National University of Defense Technology, College of Science. His research fields include optical information acquisition; transfer, storage, and processing; and spatial filter for high power laser, beam combining technologies and volume gratings designing.



**Mr Zheng Guangwei** received his MS from Air Force Engineering University in 2004. He is currently a PhD candidate at the National University of Defense Technology, College of Optoelectronic Science and Engineering, and his main research includes low-pass spatial filter design for high power laser systems.